

1    **Biotic factors dominantly determine soil inorganic carbon stock across**  
2    **Tibetan alpine grasslands**

3    Junxiao Pan <sup>a</sup>, Jinsong Wang <sup>a,\*</sup>, Dashuan Tian <sup>a</sup>, Ruiyang Zhang <sup>a</sup>, Yang Li  
4    <sup>a</sup>, Lei Song <sup>a,b</sup>, Jiaming Yang <sup>a</sup>, Chunxue Wei <sup>a</sup>, Shuli Niu <sup>a,b,\*</sup>

5    <sup>a</sup> Key Laboratory of Ecosystem Network Observation and Modeling, Institute of  
6    Geographic Sciences and Natural Resources Research, Chinese Academy of Sciences,  
7    Beijing 100101, PR China

8    <sup>b</sup> College of Resources and Environment, University of Chinese Academy of Sciences,  
9    Beijing 100049, PR China

10    \*Corresponding author at: Key Laboratory of Ecosystem Network Observation and  
11    Modeling, Institute of Geographic Sciences and Natural Resources Research, Chinese  
12    Academy of Sciences, Beijing 100101, PR China.

13    E-mail address: wangjinsong@igsnrr.ac.cn (J. Wang), sniu@igsnrr.ac.cn (S. Niu).

14

**Abstract.** Soil inorganic carbon (SIC) pool is a major component of soil C pools, and clarifying the predictors of SIC stock is urgent for decreasing soil C losses and maintaining soil health and ecosystem functions. However, the drivers and their relative effects on the SIC stock at different soil depths remain largely unexplored. Here, we conducted a large-scale sampling to investigate the effects and relative contributions of abiotic (climate and soil) and biotic (plant and microbe) drivers on the SIC stock between topsoils (0–10 cm) and subsoils (20–30 cm) across Tibetan alpine grasslands. Results showed that the SIC stock had no significant differences between the topsoil and subsoil. The SIC stock was positively associated with altitude, pH, and sand proportion, but negatively correlated with mean annual precipitation, plant aboveground biomass, plant coverage, root biomass, soil available nitrogen, microbial biomass carbon, and bacterial and fungal gene abundance. For both soil layers, biotic factors had larger effects on the SIC stock than abiotic factors did. But the relative importance of these determinants varied with soil depth, with the effects of plant and microbial variables on SIC stock weakening with soil depth, whereas the importance of climatic and edaphic variables increasing with soil depth. Specifically, bacterial and fungal gene abundance and plant coverage played dominant roles in regulating SIC stock in the topsoil, while soil pH contributed largely to the variation of SIC stock in the subsoil. Our findings highlight differential drivers over SIC stock with soil depth, which should be considered in biogeochemical models for better simulating and predicting SIC dynamics and its feedbacks to environmental changes.

## 1 Introduction

Soils store approximately 1,500 Pg of organic carbon (SOC) and 940 Pg of inorganic carbon (SIC) to a depth of 1 m (Batjes, 1996; Jobbágy & Jackson, 2000), which are the largest carbon (C) pool in the terrestrial ecosystem and play a critical part in the global C cycling (Darwish et al., 2018; Lal 2004; Prietzel et al, 2016). Compared to the relatively short turnover time of SOC, SIC has a long residence time due to soil weathering (Monger et al, 2015; Zang et al, 2018), which is considered to be fairly stable and has less contribution to changes in terrestrial ecosystem C balance (Yang et al, 2012). Therefore, previous studies have paid little attention to SIC. However, recent studies suggest that SIC is also responsive to anthropogenic activities and global climate changes such as soil acidification, atmospheric N deposition, and global warming (Yang et al, 2010; Song et al, 2022), acting as a critical C source (Liu et al, 2020) or C sink (Gao et al, 2018; Liu et al, 2021). Thus, the preservation of SIC and its roles in climate mitigation should not be neglected, especially in arid and semi-arid grasslands where store a large amount of SIC (Yang et al, 2012).

SIC stock and stability can be fundamentally altered by an array of abiotic and biotic processes (Raza et al, 2020). High precipitation can promote soil silicate minerals weathering and removal of base cations ( $\text{Ca}^{2+}$ ,  $\text{Mg}^{2+}$ ,  $\text{K}^{+}$ , and  $\text{Na}^{+}$ ) by leaching (Vicca et al, 2022). Soil acidification due to atmospheric nitrogen (N) and acid deposition and the nitrification of  $\text{NH}_4^{+}$  may greatly accelerate soil carbonate dissolution and  $\text{CO}_2$  releases (Raza et al, 2020; Song et al, 2022). Plant growth can deplete soil carbonates by releasing proton and organic acids from root rhizosphere (Goulding et al, 2016;

Kuzyakov & Razavi, 2019), and biological N<sub>2</sub> fixation by some legumes are likely to cause SIC losses (Tang et al, 1999). Furthermore, plant autotrophic and microbial heterotrophic respiration often facilitate carbonate dissolution by enhancing CO<sub>2</sub> partial pressures (An et al, 2019; Liu et al, 2021). Nevertheless, how these abiotic and biotic factors affect SIC stock and what is the relative importance of these confounding drivers remain largely uncertain.

Previous studies on SIC stock mostly have focused on the topsoil, while the patterns of SIC stock in the subsoil on a large scale remain elusive. The predictors of SIC stock in the subsoil may differ from those in the topsoil due to distinct soil microenvironments, soil physicochemical properties, root exudates, and microbial abundance and functions (Jia et al, 2017). For instance, the topsoil has larger root biomass and higher microbial activity than the subsoil, but the subsoil tends to preserve soil parent material because of the weakened weathering by the isolation of heat and energy from the surface soil (Crowther et al, 2016). Thus, the abiotic and biotic variables may exhibit different effects on SIC stock in the subsoil compared to the topsoil due to the various importance of these variables.

The Tibetan Plateau has the largest alpine grassland on the Eurasian continent, which is a vital component of global terrestrial ecosystems, providing an ideal platform to explore SIC stock and its determinants (Wang et al, 2002; Yang et al, 2010). During the past several decades, the plateau has experienced significant warming (Wang et al, 2008) and pronounced atmospheric N deposition (Liu et al, 2013; Yu et al, 2019). This continuous warming and N deposition have resulted in a significant increase in plant

growth and soil acidification (Ding et al, 2017; Yang et al, 2012), which could be likely to induce potential CO<sub>2</sub> releases from soil carbonates by biogeochemical process (Raza et al, 2020). However, a general understanding of SIC stock with soil depth across Tibetan alpine grasslands remains unexplored. Here, we researched the relative importance of climatic, edaphic, plant, and microbial variables to SIC stock at different soil layers along an approximately 3,000 km transect of alpine grasslands on the Tibetan Plateau, spanning a broad range of climatic and geographical conditions. Specifically, two key questions are addressed in this study: (1) what are the differences of SIC stock between the topsoil and subsoil? (2) how does the relative importance of climatic, edaphic, plant, and microbial variables to the variation of SIC stock along with soil depth?

## 93    **2 Material and methods**

### 94    **2.1 Study area and field sampling**

95    During July, August, and September 2020, we conducted large-scale systematic field  
96    surveys and samplings in Tibetan alpine grasslands. The total 25 sampling sites covered  
97    approximately 3,000 km and included three grassland types (i.e, 11 alpine meadow, 8  
98    alpine steppe, and 6 alpine desert sites). The distance between nearby sampling sites  
99    was about 120 km. The study sites cover a broad geographic and climatic range, with  
100    longitude and latitude ranging from 79°49'39" to 102°25'31" E and 31°06'37" to  
101    32°43'09" N, respectively, and the altitude ranging from 3500 m to 5016 m. These sites  
102    covered a broad precipitation gradient varying between 72 mm and 706 mm. The mean  
103    annual temperature (MAT) ranged from −3.9°C to 5.8°C. The plant communities were  
104    dominated by *Kobresia tibetica* Maxim, *Stipa caucasica*, *Kobresia pygmaea*, *Stipa*  
105    *purpurea*, and *Leontopodium pusillum*. Soils were *Cambisol* and some were loess-  
106    derived *Luvisol*. The site location, grassland type, climatic, and plant parameters were  
107    detailed in Table S1.

### 108    **2.2 Climatic data**

109    The climatic data were derived from the LPSDC (Loess Plateau Scientific Data Center,  
110    <http://loess.geodata.cn/>) (Peng et al, 2019). The Kriging interpolation was conducted to  
111    obtain spatial distributions of 30-year MAT and MAP (1987-2017) at each sampling  
112    site by a geographic coordinate system.

### 2.3 Soil properties

At each site, we selected four 1 m × 1 m plots for soil and plant samplings and the distance between nearby sampling plots was 25 m. In each plot, a 7.5-cm diameter soil drill was used to take five soil cores at fixed soil depths (0-10 cm, 10-20 cm, and 20-30 cm), and a 2-mm mesh was used to remove stones. We used soil samples from 0–10 cm and 20–30 cm to represent the topsoil and subsoil, respectively, according to previous studies (Angst et al, 2021; Rumpel & Kögel-Knabner 2011; Zhou et al., 2021). After mixing, 100 g of fresh soils from each plot were collected and stored in a –4°C portable icebox, then returned to the laboratory and stored at –20°C for microbial properties. The rest soil samples about 700 g were also sent back to the laboratory and air-dried for measurements of other soil properties. A 40 cm × 40 cm × 40 cm (length × width × depth) pit was dug for measuring soil bulk density (BD) by using a constant volume soil sampling drill (100 cm<sup>3</sup>), and the undisturbed soil was preserved in aluminum specimen boxes returning to the laboratory and oven-dried for 48 hours at 105°C and weighed. The oven-dried soil (20 g) was screened into gravel by sifting through a 2-mm mesh sieve and gravels larger than 2 mm were collected and weighed to determine the percentage of gravels. Soil pH (1:25 soil: H<sub>2</sub>O) was measured using a soil pH meter, and available nitrogen (AN) was determined by the alkaline-hydrolysis diffusion method. A laser particle analyzer (Mastersizer 2000, Malvern Panalytical, UK) was applied to measure soil mechanical compositions, including clay (< 2 μm), silt (2-50 μm), and sand (> 50 μm) proportion. SIC was determined by using an inorganic C analyzer (multi EA® 4000; Analytic Jena, Germany). The multi EA 4000 C elemental

analyzer was equipped with the automatic TIC solids module and calibrated before the analysis. The sample boat was acidified automatically with 40 %  $\text{H}_3\text{PO}_4$  in the reactor of the TIC module. And the  $\text{CO}_2$  from the carbonate was released, the measuring gas was dried and cleaned and the carbon content was measured by means of the wide-range NDIR detector. Before being analyzed directly, all soil samples were ground into solid fine powders with a mortar, and for the determination of TIC, a standard, prepared by solids-dilution of  $\text{CaCO}_3$  with  $\text{SiO}_2$  (0.2 % C), was used, with weighting range 7-200 mg, to cover a wide concentration range.

## **2.4 Plant properties**

In each plot, we estimated plant coverage (PC) by the projection method, namely the proportion of vegetation projection to the area of the sampling plot. In addition, plant aboveground biomass and belowground roots were clipped and collected, respectively, then oven-dried at 60°C and weighed to determine plant aboveground biomass (PAB) and root biomass (RB).

## **2.5 Microbial attributes**

Soil microbial biomass carbon (MBC) was measured by using a chloroform fumigation-extraction procedure (Brookes et al, 1985). Briefly, 10 g of unfumigated and chloroform-fumigated fresh soil samples were extracted by using 0.5 M  $\text{K}_2\text{SO}_4$  after 24 h of incubation, respectively. Then, the extracts were analyzed by using a TOC analyzer (multi N/C® 3100; Analytic Jena, Germany). The MBC was determined by



the differences in C concentrations between unfumigated and chloroform-fumigated samples, and the correction factor (i.e, KC= 0.45) was used to convert microbial C to MBC (Joergensen, 1996).

Real-time polymerase chain reaction (qPCR) was used to quantify bacterial (BA) and fungal gene abundance (FA) by the absolute quantification method based on the gene copy number (Tatti et al, 2016). Each reaction was carried out 3 times with a mixture of a total 20 µL volume, including 2 µL of DNA template, 10 µL of 2× ChamQ SYBR Color qPCR Master Mix, and 0.4 µL (5µM concentration) each of forward and reverse primer specific for each gene. And the PCR conditions were 95°C for 5 min, then 40 cycles for the 18S rRNA gene and 16S rRNA gene. Each cycle involved melting at 95°C for 30 s, annealing at 55°C for 30 s, an extension of 72°C for 40 s, and finally 10°C until terminated. And the primer pair SSU0817/1196 and Eub338/Eub806 were used for amplifying fungi and bacteria in PCR amplification, respectively. Then the DNA concentration was determined by using a QuantiFluor™-ST fluorescent quantitative system (Promega, Fitchburg, WI, USA). The abbreviations of all variables were detailed in Table S2.

## 2.6 Statistical analyses

The total SIC density (C stock per land area) in each soil depth layer was calculated using Equation (1) (Pan et al, 2019):

$$\text{SIC density (g C m}^{-2}\text{)} = \text{SIC (g C kg}^{-1}\text{)} \times \text{BD (g cm}^{-3}\text{)} \times \text{d (cm)} \times (1-\text{g}) / 100 \quad (1)$$

where SIC is soil inorganic C content,  $d$  is the depth of the soil layer (0.1 m),  $BD$  is bulk density, and  $g$  is the percentage of gravel fraction ( $>2$  mm).

First, the differences of SIC stock and corresponding abiotic and biotic variables between the topsoil and subsoil were examined by  $T$ -test. Second, SIC density and various abiotic and biotic variables were log-transformed and standardized (z-score normalization) to perform the assumption of normality and homogeneity by Shapiro-Wilk and Levene's test, respectively (Pan et al, 2021). Then the linear regressions were used to test SIC density about different variables for both the topsoil and subsoil across sites.

Third, a linear model was employed to examine SIC density with abiotic and biotic variables by using the maximum likelihood estimation with the `lm` package. And the relative effect of the parameter estimates was calculated to evaluate the relative importance of drivers controlling SIC density. Also, SIC density and abiotic and biotic variables were standardized before analyses, using the Z-score to interpret variable estimates on a comparable scale (Gross et al, 2017).

$$\text{Log (SIC density)} = \beta_0 + \beta_1 \log X_1 + \beta_2 \log X_2 + \dots + \beta_{12} \log X_{12} \quad (2)$$

where  $\beta_0$  and  $\beta_i$  ( $i=1, 2, 3 \dots 12$ ) are intercept and coefficients, respectively. To explore the determinants of SIC density in different soil depths across all sites, the absolute values of slopes of the variables were extracted and plotted. Then, 12 controlling variables were categorized into four groups, including climatic (MAP, MAT, and altitude), edaphic (pH, AN, and sand proportion), plant (PB, PC, and RB), and

196 microbial (MBC, BA, and FA) factors, to quantify their relative contribution to SIC  
197 density (Fang et al, 2019).

198 Furthermore, the relative importance of abiotic (climatic and edaphic) and biotic  
199 (plant and microbial) variables in determining SIC density was quantified by  
200 performing variation partitioning analyses (VPA) by using the “vegan” package in R  
201 4.1.3.

202

## 3 Results

### 3.1 SIC density and influencing variables in different soil depths

SIC density and SIC content had no significant differences between the topsoil and subsoil, but bulk density in the subsoil was much higher compared with the topsoil. Specifically, SIC density in the topsoil and subsoil ranged from 1.8 g C m<sup>-2</sup> to 3271 g C m<sup>-2</sup> and 5.4 g C m<sup>-2</sup> to 3214 g C m<sup>-2</sup> across 25 sampling sites, with an average of 802 ± 220 g C m<sup>-2</sup> and 814 ± 236 g C m<sup>-2</sup>, respectively (Fig. 1). No significant changes in SIC density with soil depth were observed in both the alpine steppe and alpine desert ( $p=0.113$  and  $p=0.068$ , respectively; Fig. 1), but SIC density was higher in the subsoil than that in the topsoil in the alpine meadow ( $p = 0.002$ , Fig. 1).

Meanwhile, the majority of abiotic and biotic drivers had significant differences between the topsoil and subsoil (Table 1). RB, AN, MBC, BA, and FA in the topsoil were significantly larger than those in the subsoil (all  $p<0.001$ ). In contrast, pH was significantly lower in the topsoil than in the subsoil ( $p<0.001$ , Table 1). However, the sand proportion between the two soil depths had no significant differences (Table 1).

### 3.2 Associations of SIC density with abiotic and biotic variables

The SIC density was closely related to multiple abiotic and biotic variables (Figs 2 and 3). For both the topsoil and subsoil, the SIC density was positively associated with altitude, pH, and sand proportion, but negatively correlated with MAP, PAB, PC, RB, AN, BA, and FA. The SIC density showed a negative correlation with MBC in the

topsoil (Fig. 2), but not in the subsoil (Fig. 3). Meanwhile, the SIC density in both two soil depths did not correlate with MAT (Figs. 2 and 3).

### **3.3 Determinants of SIC density in different soil depths**

The linear model and VPA collectively displayed that the predominant drivers of SIC density differed with soil depth (Figs. 4 and 5). Specifically, for the topsoil, the linear model revealed that microbial and plant variables largely explained the variations in the SIC density, followed by edaphic variables and climate contributed the least (Fig. 4). Among these variables, PC, BA, and FA exhibited larger effects on the SIC density compared with other controlling factors (Fig. 4). Also, the VPA analysis illustrated that biotic factors explained the majority variation of SIC density compared with abiotic factors (Fig. 5). For the subsoil, the linear model showed that edaphic variables largely explained the variation in SIC density, followed by microbial and plant variables, and climate contributed the least (Fig. 4). Among these variables, the soil pH had larger contributions to the variation of SIC density rather than others (Fig. 4). Meanwhile, the VPA analysis confirmed that the effects of biotic factors on SIC density were larger than those of abiotic factors in the subsoil (Fig. 5).

## 4 Discussion

To the best of our knowledge, this study was the first to afford large-scale evidence of the relative contribution of abiotic and biotic drivers to the variation of SIC stock at different soil depths, which has considerable implications for grasping the importance of SIC in the ecosystem C cycling. Since considerably stable characteristics and the long turnover time (Mi et al, 2008; Yang et al, 2010; Zamanian et al, 2018), SIC stock is traditionally considered to be dominated by abiotic factors including soil moisture, soil pH, CO<sub>2</sub> partial pressure, and Ca<sup>2+</sup> concentrations according to the equilibrium of carbonate precipitation–dissolution reactions ( $\text{CaCO}_3 + \text{H}_2\text{O} + \text{CO}_2 \rightarrow \text{Ca}^{2+} + 2\text{HCO}_3^-$  and  $\text{Ca}^{2+} + 2\text{HCO}_3^- \rightarrow \text{CaCO}_3 + \text{H}_2\text{O} + \text{CO}_2$ ) and mineral carbonation ( $\text{MgSiO}_4 + 2\text{CO}_2 \rightarrow 2\text{MgCO}_3 + \text{SiO}_2$  and  $\text{CaMgSi}_2\text{O}_6 + \text{CO}_2 + \text{H}_2\text{O} \rightarrow \text{Ca}_2\text{Mg}_5\text{Si}_8\text{O}_{22}(\text{OH})_2 + \text{CaCO}_3 + \text{SiO}_2$ ) (Mi et al, 2008; Rey, 2015; Yang et al, 2012; Yang and Yang, 2020). These abiotic factors were proved to have large impacts on the dissolution and deposition processes of inorganic C and ultimately determined the reservation and distribution of SIC (Rey, 2015; Rowley et al, 2018).

However, many biological processes and factors were not quantitatively considered in previous studies. In this study, based on the approach of large-scale field samplings across Tibetan alpine grasslands, we estimated the predominant drivers of SIC stock in the topsoil and subsoil. Our results found the predominant roles of microbial and plant factors in determining SIC stock in both topsoil and subsoil. More importantly, the effects of biotic factors on SIC stock weakened with soil depth (Fig. 4). These results were different from those demonstrating the critical influence of abiotic processes on

SIC stock (Mi et al, 2008; Yang et al, 2010).

We found that increasing plant aboveground biomass, plant coverage, and root biomass significantly decreased SIC density (Figs. 2 and 3). Plant factors could contribute to the decline of SIC stock by three pathways including uptakes of exchangeable cations, plant organic matter inputs, and rhizosphere processes. First, a large decline in soil base cations is likely to be induced by plant uptake with increasing plant biomass. And the losses of soil exchangeable base cations can cause the transformation of SIC to CO<sub>2</sub>, which is ultimately released into the atmosphere (Huang et al, 2015). Second, increasing plant residue inputs can enhance carbonic and organic acid production into soil water solution via microbial decomposition, which reduces the availability of soil base cations through cation exchange in the soil (Sartori et al, 2007) and increase the dissolution and leaching of carbonates, resulting in a decrease in the SIC. Third, the plant rhizosphere effect on releasing CO<sub>2</sub> from carbonates should not be ignored, especially in alkaline soils. By releasing organic acids and protons as well as CO<sub>2</sub>, plant roots can reduce soil pH and increase CO<sub>2</sub> in the rhizosphere (Lenzewski et al, 2018), both of which dissolve carbonates by neutralization (Harley & Gilkes, 2000). In addition, organic compounds from plant root exudates, such as malate or citrate, can stimulate mineral weathering by dissolving silicate minerals (Dontsova et al, 2020).

Furthermore, the topsoil has a larger quantity and higher quality of plant residues than the subsoil, which indicates a more potential for carbonate dissolution by biological processes for the surface soil (Liu et al, 2020). The large root biomass in the

topsoil can increase the uptake of base cations and result in increasing proton and organic acids in root exudates (Li et al, 2007), thus reducing the soil carbonate content for maintaining the charge balance. In addition, the larger plant roots exuded more organic compounds in the topsoil that can stimulate parent mineral weathering and dissolve silicate minerals by chelating reaction products (Doetterl et al, 2015; Dontsova et al, 2020).

Previous studies reported that microbial properties may not be important in mediating SIC accumulation (Liu et al, 2021; Wang et al, 2015). However, our results found that microbial factors including microbial biomass and bacterial and fungal gene abundance showed significant and negative associations with SIC stock (Figs. 2 and 3), which could be due to microbes driving the carbonate dissolution processes, including microbial respiration, organic matter mineralization, and releases of proton and organic acids by microbial metabolic activity. First, the increase in microbial respiration can improve CO<sub>2</sub> production and enhance the partial pressure of CO<sub>2</sub>, leading to a decline in pH and further dissolution of carbonates (Chang et al, 2012). In addition, soil organic matter mineralization and litter decomposition by microbes can induce the dissolution of CO<sub>2</sub> and the release of organic acids (Goulding, 2016; Kuzyakov & Razavi, 2019), both of which decrease the SIC stock. Meanwhile, chelates and enzymes excreted by microbes may contribute to enhancing mineral dissolution rates and organic matter decomposition (Xiao et al, 2015; Zaharescu et al, 2020).

We also revealed that bacterial and fungal gene abundance contributed significantly to the variation of SIC stock (Figs. 2 and 3), which was likely to account for decreasing



soil pH in the involvement of microbial biological reactions. For instance, nitrifying bacteria can oxidize ammonium to nitrate ( $\text{NH}_4^+ + \text{OH}^- + 2\text{O}_2 \rightarrow \text{NO}_3^- + 2\text{H}_2\text{O} + \text{H}^+$ ), and the production of acidity is finally neutralized through accelerating carbonate dissolution (Zamanian et al, 2016). Also, some nitrogen-fixing bacteria that lived in symbiosis with leguminous plants can acidify the soil by excreting protons during  $\text{N}_2$  fixation (Vicca et al, 2022). Furthermore, fungi are likely to accelerate carbonate neutralization by exuding protons and organic acids (Van Hees et al, 2006; Wild et al, 2021).

Microbial factors also affected SIC stock more in the topsoil than in the subsoil. The large plant residues incorporated into the topsoil provided substantial amounts of organic matter for microbial living and decomposition (Oelkers et al, 2015; Ven et al, 2020), which can stimulate microbial abundance and activities and promote microbial extracellular enzymes. These extracellular excretions play a fundamental role in microbial respiration and  $\text{CO}_2$  production, both of which stimulate silicate weathering and carbonate dissolution (Vicca et al, 2022). Meanwhile, the higher  $\text{CO}_2$  flux and  $\text{CO}_2$  partial pressure resulting from the biological activities of roots and soil microorganisms in the topsoil could enhance carbonate dissolution and formations of pedogenic inorganic C (Chang et al, 2012; Zamanian et al, 2016).

Different from plant and microbial factors, the effects of edaphic factors on SIC stock strengthened with soil depth, with soil pH being the most important predictor among edaphic variables (Fig. 4). The buffering capacity in soil solutions determines the equilibrium of ion inputs and outputs by soil pH (Huang et al, 2015). In this study,

soil pH in the subsoil (7.85) was much higher than that (7.66) in the topsoil (Table 1). The higher pH could buffer the replacement of the exchangeable cations with protons (Frank & Stuanes, 2003) and increase the preservation of base cations (Gandois et al, 2011). Given that base cations and carbonates provide the major buffering capacity in the alkaline soil (Yang et al, 2012), the topsoil could be subject to a larger loss of base cations and SIC due to the lower soil pH compared to the subsoil.

Taken together, our results revealed that SIC stock was closely linked with biotic factors, which highlights the roles of biological processes in regulating SIC dynamics (Hong et al, 2019). These results imply that the widespread enhancement of vegetation productivity under global environmental changes (e.g, warming and rewetting) (Ding et al, 2017; Wang et al, 2008) may aggravate the depletion of SIC stock (Raza et al, 2020). Meanwhile, previous studies have urged the need for incorporating microbial processes and indicators into Earth system models (ESMs) to reduce the uncertainty in predicting soil C dynamics, especially SOC decomposition (Allison et al, 2010; Moorhead and Sinsabaugh, 2006; Todd-Brown et al, 2013). However, our findings highlighted the vital role of microbial factors in regulating soil C balance from inorganic C preservation. Thus, incorporating microbial processes into the models can aid in the understanding of overall soil C responses, because SOC and SIC are formed, protected, and lost in different ways.

More importantly, the effects of biotic factors on SIC stock weakened with soil depth, which implies that SIC may be susceptible to environmental changes in the topsoil where is the hotspot of root and microbial activities. Even though biotic factors

in the subsoil played less roles in affecting SIC stock compared with the topsoil, an increase in rooting depth is expected in response to climate warming and land-use change (Liu et al. 2018), which is likely to cause SIC losses in the deep soil by root growth. Therefore, it is a necessity to further explore the effects of biotic factors on SIC stock in the deep soil in the context of global changes. Overall, the contribution of SIC to CO<sub>2</sub> is not ignored and SIC maintenance has a considerable significance on soil C losses and maintains the health and ecosystem functions (Raza et al, 2020; Zamanian et al, 2018). Our study provides robust evidence that biotic factors are mainly responsible for the variation of SIC stock and that topsoils and subsoils should be considered separately when modeling SIC dynamics and its feedbacks on climate change (Yang et al, 2012; Zamanian & Kuzyakov, 2019).

## **5 Conclusions**

Our findings showed that the climatic, edaphic, plant, and microbial variables jointly affected SIC stock in the Tibetan grasslands and that biotic factors had a larger contribution than abiotic factors to the variation of SIC stock. Furthermore, the effects of microbial and plant variables on SIC stock weakened with soil depth, while the effects of edaphic variables strengthened with soil depth. The contrasting responses and drivers of SIC stock between the topsoil and subsoil highlight differential mechanisms underlying SIC preservation with soil depth, which is crucial to understanding and predicting SIC dynamics and its feedbacks to environmental changes.

**Data availability.**

The data that support the findings of this study are available from the corresponding author upon reasonable request.

**Supplement.**

Supporting information is also available as supplementary material.

**Author contributions.**

JP, JW, and SN designed the study. JP, JW, DT, RZ, YL, LS, JY, CW, and SN were involved in drafting or revising the manuscript. All authors read and approved the final manuscript.

**Competing interests.**

The authors declare that they have no conflict of interest.

**Acknowledgments**

This study was financially supported by the Second Tibetan Plateau Scientific Expedition and Research (STEP) program (2019QZKK0302), the National Natural Science Foundation of China (31988102 and 32101390), and the China National Postdoctoral Program for Innovative Talents (BX20200330).

## References

- Allison, S. D., Wallenstein, M. D., Bradford, M. A.: Soil-carbon response to warming dependent on microbial physiology, *Nat. Geosci.*, 3(5), 336-340, <https://doi.org/10.1038/NGEO846>, 2010.
- An, H., Wu, X. Z., Zhang, Y. R., Tang, Z. S.: Effects of land-use change on soil inorganic carbon: A meta-analysis, *Geoderma*, 353, 273-282, <https://doi.org/10.1016/j.geoderma.2019.07.008>, 2019.
- Angst, G., Mueller, K. E., Nierop, K., Simpson, M. J.: Plant- or microbial-derived? A review on the molecular composition of stabilized soil organic matter, *Soil Biol. Biochem.*, 156, <https://doi.org/10.1016/j.soilbio.2021.108189>, 2021.
- Batjes, N. H.: Total carbon and nitrogen in the soils of the world, *Eur. J. Soil Sci.*, 47(2), 151-163. <https://doi.org/10.1111/j.1365-2389.1996.tb01386.x>, 1996.
- Brookes, P. C., Landman, A., Pruden, G., Jenkinson, D. S.: Chloroform fumigation and the release of soil -nitrogen- A rapid direct extraction method to measure microbial biomass nitrogen in soil, *Soil Biol. Biochem.*, 17(6), 837-842, [https://doi.org/10.1016/0038-0717\(85\)90144-0](https://doi.org/10.1016/0038-0717(85)90144-0), 1985.
- Chang, R. Y., Fu, B. J., Liu, G. H., Wang, S., Yao, X. L.: The effects of afforestation on soil organic and inorganic carbon: A case study of the Loess Plateau of China, *Catena*, 95, 145-152, <https://doi.org/10.1016/j.catena.2012.02.012>, 2012.
- Crowther, T. W., Todd-Brown, K., Rowe, C. W., Wieder, W. R., Carey, J. C., Machmuller, M. B., Snoek, B. L., Fang, S., Zhou, G., Allison, S. D., Blair, J. M., Bridgham, S. D., Burton, A. J., Carrillo, Y., Reich, P. B., Clark, J. S., Classen, A.

408 T., Dijkstra, F.A., Elberling, B., Emmett, B.A., Estiarte, M., Frey, S. D., Guo, J.,  
 409 Harte, J., Jiang, L., Johnson, B.R., Kroel-Dulay, G., Larsen, K. S., Laudon, H.,  
 410 Lavallee, J. M., Luo, Y., Lupascu, M., Ma, L. N., Marhan, S., Michelsen, A., Mohan,  
 411 J., Niu, S., Pendall, E., Penuelas, J., Pfeifer-Meister, L., Poll, C., Reinsch, S.,  
 412 Reynolds, L.L., Schmidt, I. K., Sistla, S., Sokol, N. W., Templer, P. H., Treseder,  
 413 K. K., Welker, J. M., Bradford, M. A.: Quantifying global soil carbon losses in  
 414 response to warming, *Nature*, 540(7631), 104, <https://doi.org/10.1038/nature20150>,  
 415 2016.

416 Darwish, T., Atallah, T., Fadel, A.: Challenges of soil carbon sequestration in the  
 417 NENA region, *SOIL*, 4, 225-235, <https://doi.org/10.5194/soil-4-225-2018>, 2018.

418 Ding, J. Z., Chen, L. Y., Ji, C. J., Hugelius, G., Li, Y. N., Liu, L., ; Qin, S. Q., Zhang,  
 419 B. B., Yang, G. B., Li, F., Fang, K., Chen, Y. L., Peng, Y. F., Zhao, X., He, H. L.,  
 420 Smith, P., Fang, J. Y., Yang, Y. H.: Decadal soil carbon accumulation across Tibetan  
 421 permafrost regions, *Nat. Geosci.*, 10(6), 420, <https://doi.org/10.1038/NGEO2945>,  
 422 2017.

423 Doetterl, S., Berhe, A. A., Arnold, C., Bode, S., Fiener, P., Finke, P., Fuchslueger, L.,  
 424 Griepentrog, M., Harden, J. W., Nadeu, E., Schnecker, J., Six, J., Trumbore, S., Van  
 425 Oost, K., Vogel, C., Boeckx, P.: Links among warming, carbon and microbial  
 426 dynamics mediated by soil mineral weathering, *Nat. Geosci.*, 11(8), 589,  
 427 <https://doi.org/10.1038/s41561-018-0168-7>, 2018.

428 Dontsova, K., Balogh-Brunstad, Z., Chorover, J.: Plants as drivers of rock weathering.  
 429 In K. Dontsova, Z. Balogh-Brunstad, G. L. Roux (Eds.), *Biogeochemical cycles* (pp.

33–58), John Wiley Sons, Inc, 2020.

Fang, K., Qin, S. Q., Chen, L. Y., Zhang, Q. W., Yang, Y. H.: Al/Fe mineral controls on soil organic carbon stock across Tibetan alpine grasslands, *J. Geophys. Res.-Biogeo.*, 124(2), 247-259, <https://doi.org/10.1029/2018JG004782>, 2019.

Frank, J., Stuanes, A. O.: Short-term effects of liming and vitality fertilization on forest soil and nutrient leaching in a Scots pine ecosystem in Norway, *Forest Ecol. Manag.*, 176(1-3), 371-386, [https://doi.org/10.1016/S0378-1127\(02\)00285-2](https://doi.org/10.1016/S0378-1127(02)00285-2), 2003.

Gandois, L., Perrin, A. S., Probst, A.: Impact of nitrogenous fertiliser-induced proton release on cultivated soils with contrasting carbonate contents: A column experiment, *Geochimica et Cosmochimica Acta*, 75(5), 1185-1198, <https://doi.org/10.1016/j.gca.2010.11.025>, 2011.

Gao, Y., Dang, P., Zhao, Q. X., Liu, J. L., Liu, J. B.: Effects of vegetation rehabilitation on soil organic and inorganic carbon stocks in the Mu Us Desert, northwest China, *Land Degrad. Dev.*, 29(4), 1031-1040, <https://doi.org/10.1002/ldr.2832>, 2018.

Goulding, K.: Soil acidification and the importance of liming agricultural soils with particular reference to the United Kingdom, *Soil Use Manag.*, 32(3), 390-399, <https://doi.org/10.1111/sum.12270>, 2016.

Gross, N., Le Bagousse-Pinguet, Y., Liancourt, P., Berdugo, M., Gotelli, N. J., Maestre, F. T.: Functional trait diversity maximizes ecosystem multifunctionality, *Nat. Ecol. Evol.*, 1(5), <https://doi.org/10.1038/s41559-017-0132>, 2017.

Harley, A. D., Gilkes, R. J.: Factors influencing the release of plant nutrient elements from silicate rock powders: a geochemical overview. *Nutri. Cycl. Agroecosyst.*,

452 56(1), 11-36, <https://doi.org/10.1023/A:1009859309453>, 2000.

453 Hong, S. B., Gan, P., Chen, A. P.: Environmental controls on soil pH in planted forest  
 454 and its response to nitrogen deposition, *Environ. Res.*, 172, 159-165,  
 455 <https://doi.org/10.1016/j.envres.2019.02.020>, 2019.

456 Huang, P., Zhang, J. B., Xin, X. L., Zhu, A. N., Zhang, C. Z., Ma, D. H., Zhu, Q. G.,  
 457 Yang, S., Wu, S. J.: Proton accumulation accelerated by heavy chemical nitrogen  
 458 fertilization and its long-term impact on acidifying rate in a typical arable soil in the  
 459 Huang-Huai-Hai Plain, *J. Integr. Agr.*, 14(1), 148-157,  
 460 [https://doi.org/10.1016/S2095-3119\(14\)60750-4](https://doi.org/10.1016/S2095-3119(14)60750-4), 2015.

461 Jia, J., Feng, X. J., He, J. S., He, H. B., Lin, L., Liu, Z. G.: Comparing microbial carbon  
 462 sequestration and priming in the subsoil versus topsoil of a Qinghai-Tibetan alpine  
 463 grassland, *Soil Biol. Biochem.*, 104, 141-151,  
 464 <https://doi.org/10.1016/j.soilbio.2016.10.018>, 2017.

465 Jobbagy, E. G., Jackson, R. B.: The vertical distribution of soil organic carbon and its  
 466 relation to climate and vegetation, *Ecol. Appl.*, 10(2), 423-436,  
 467 <https://doi.org/10.2307/2641104>, 2000.

468 Joergensen, R. G.: The fumigation-extraction method to estimate soil microbial  
 469 biomass: Calibration of the k(EC) value, *Soil Biol. Biochem.*, 28(1), 25-31,  
 470 [https://doi.org/10.1016/0038-0717\(95\)00102-6](https://doi.org/10.1016/0038-0717(95)00102-6), 1996.

471 Kuzyakov, Y., Razavi, B. S.: Rhizosphere size and shape: Temporal dynamics and  
 472 spatial stationarity, *Soil Biol. Biochem.*, 135, 343-360,  
 473 <https://doi.org/10.1016/j.soilbio.2019.05.011>, 2019.



474 Lal, R.: Soil carbon sequestration impacts on global climate change and food security,  
 475 Science, 304(5677), 1623-1627, <https://doi.org/10.1126/science.1097396>, 2004.

476 Lenzewski, N., Mueller, P., Meier, R. J., Liebsch, G., Jensen, K., Koop-Jakobsen, K.:  
 477 Dynamics of oxygen and carbon dioxide in rhizospheres of *Lobelia dortmanna* - a  
 478 planar optode study of belowground gas exchange between plants and sediment,  
 479 New Phytol., 218(1), 131-141, <https://doi.org/10.1111/nph.14973>, 2018.

480 Li, L., Li, S. M., Sun, J. H., Zhou, L. L., Bao, X. G., Zhang, H. G., Zhang, F. S.:  
 481 Diversity enhances agricultural productivity via rhizosphere phosphorus facilitation  
 482 on phosphorus-deficient soils, Proc. Natl. Acad. Sci. U. S. A., 104(27), 11192-  
 483 11196, <https://doi.org/10.1073/pnas.0704591104>, 2007.

484 Liu, H. Y., Mi, Z. R., Lin, L., Wang, Y. H., Zhang, Z. H., Zhang, F. W., Wang, H. Liu,  
 485 L. L., Zhu, B., Cao, G. M., Zhao, X. Q., Sanders, N. J., Classen, A. T., Reich, P. B.,  
 486 He, J. S.: Shifting plant species composition in response to climate change stabilizes  
 487 grassland primary production, Proc. Natl. Acad. Sci. U. S. A., 115(16), 4051-4056,  
 488 <https://doi.org/10.1073/pnas.1700299114>, 2018.

489 Liu, S. S., Zhou, L. H., Li, H., Zhao, X., Yang, Y. H., Zhu, Y. K., ... Fang, J. Y.: Shrub  
 490 encroachment decreases soil inorganic carbon stocks in Mongolian grasslands, J.  
 491 Ecol., 108(2), 678-686, <https://doi.org/10.1111/1365-2745.13298>, 2020.

492 Liu, X. J., Zhang, Y., Han, W. X., Tang, A. H., Shen, J. L., Cui, Z. L., Vitousek, P.,  
 493 Erismann, J. W., Goulding, K., Christie, P., Fangmeier, A., Zhang, F. S.: Enhanced  
 494 nitrogen deposition over China, Nature, 494(7438), 459-462,  
 495 <https://doi.org/10.1038/nature11917>, 2013.

496 Liu, Z., Sun, Y. F., Zhang, Y. Q., Feng, W., Lai, Z. R., Qin, S. G.: Soil microbes  
 497 transform inorganic carbon into organic carbon by dark fixation pathways in desert  
 498 soil. *J. Geophys. Res. Biogeosciences*, 126(5),  
 499 <https://doi.org/10.1029/2020JG006047>, 2021.

500 Mi, N., Wang, S. Q., Liu, J. Y., Yu, G. R., Zhang, W. J., Jobbaagy, E.: Soil inorganic  
 501 carbon storage pattern in China, *Glob. Chang. Biol.*, 14(10), 2380-2387,  
 502 <https://doi.org/10.1111/j.1365-2486.2008.01642.x>, 2008.

503 Monger, H. C., Kraimer, R. A., Khresat, S., Cole, D. R., Wang, X. J., Wang, J. P.:  
 504 Sequestration of inorganic carbon in soil and groundwater, *Geology*, 43(5), 375-378,  
 505 <https://doi.org/10.1130/G36449.1>, 2015.

506 Moorhead, D. L., Sinsabaugh, R. L.: A theoretical model of litter decay and microbial  
 507 interaction, *Ecol. Monogr.*, 76(2), 151-174, [https://doi.org/10.1890/0012-](https://doi.org/10.1890/0012-9615(2006)076[0151:ATMOLD]2.0.CO;2)  
 508 [9615\(2006\)076\[0151:ATMOLD\]2.0.CO;2](https://doi.org/10.1890/0012-9615(2006)076[0151:ATMOLD]2.0.CO;2), 2006.

509 Oelkers, E. H., Benning, L. G., Lutz, S., Mavromatis, V., Pearce, C. R., Plummer, O.:  
 510 The efficient long-term inhibition of forsterite dissolution by common soil bacteria  
 511 and fungi at Earth surface conditions, *Geochim. Cosmochim. Acta*, 168, 222-235,  
 512 <https://doi.org/10.1016/j.gca.2015.06.004>, 2015.

513 Pan, J. X., Wang, J. S., Zhang, R. Y., Tian, D. S., Cheng, X. L., Wang, S., Chen, C.,  
 514 Yang, L., Niu, S. L.: Microaggregates regulated by edaphic properties determine the  
 515 soil carbon stock in Tibetan alpine grasslands, *Catena*, 206,  
 516 <https://doi.org/10.1016/j.catena.2021.105570>, 2021.

517 Pan, J. X., Zhang, L., He, X. M., Chen, X. P., Cui, Z. L.: Long-term optimization of

518 crop yield while concurrently improving soil quality, *Land Degrad. Dev.*, 30(8),  
519 897-909, <https://doi.org/10.1002/ldr.3276>, 2019.

520 Peng, S. Z., Ding, Y. X., Liu, W. Z., Li, Z.: 1 km monthly temperature and precipitation  
521 dataset for China from 1901 to 2017, *Earth Syst. Sci. Data*, 11(4), 1931-1946,  
522 <https://doi.org/10.5194/essd-11-1931-2019>, 2019.

523 Prietzel, J., Zimmermann, L., Schubert, A., Christophel, D.: Organic matter losses in  
524 German Alps forest soils since the 1970s most likely caused by warming, *Nat.*  
525 *Geosci.*, 9(7), 543, <https://doi.org/10.1038/NGEO2732>, 2016.

526 Raza, S., Miao, N., Wang, P. Z., Ju, X. T., Chen, Z. J., Zhou, J. B., Kuzyakov, Y.:  
527 Dramatic loss of inorganic carbon by nitrogen-induced soil acidification in Chinese  
528 croplands, *Glob. Chang. Biol.*, 26(6), 3738-3751, <https://doi.org/10.1111/gcb.15101>,  
529 2020.

530 Rey, A.: Mind the gap: non-biological processes contributing to soil CO<sub>2</sub> efflux, *Glob.*  
531 *Chang. Biol.*, 21(5), 1752-1761, <https://doi.org/10.1111/gcb.12821>, 2015.

532 Rowley, M. C., Grand, S., Verrecchia, E. P.: Calcium-mediated stabilisation of soil  
533 organic carbon, *Biogeochemistry*, 137(1-2), 27-49, [https://doi.org/10.1007/s10533-](https://doi.org/10.1007/s10533-017-0410-1)  
534 [017-0410-1](https://doi.org/10.1007/s10533-017-0410-1), 2018.

535 Rumpel, C., Kogel-Knabner, I.: Deep soil organic matter-a key but poorly understood  
536 component of terrestrial C cycle, *Plant Soil*, 338(1-2), 143-158,  
537 <https://doi.org/10.1007/s11104-010-0391-5>, 2011.

538 Sartori, F., Lal, R., Ebinger, M. H., Eaton, J. A.: Changes in soil carbon and nutrient  
539 pools along a chronosequence of poplar plantations in the Columbia Plateau, Oregon,

540 USA, Agric. Ecosyst. Environ., 122(3), 325-339,  
541 <https://doi.org/10.1016/j.agee.2007.01.026>, 2007.

542 Song, X. D., Yang, F., Wu, H. Y., Zhang, J., Li, D. C., Liu, F., Zhao, Y. G., Yang, J.  
543 L., Ju, B., Cai, C. F., Huang, B. A., Long, H. Y., Lu, Y., Sui, Y. Y., Wang, Q. B.,  
544 Wu, K. N., Zhang, F. R., Zhang, M. K., Shi, Z., Ma, W. Z., Xin, G., Qi, Z. P.,  
545 Chang, Q. R., Ci, E., Yuan, D. G., Zhang, Y. Z., Bai, J. P., Chen, J. Y., Chen, J.,  
546 Chen, Y. J., Dong, Y. Z., Han, C. L., Li, L., Liu, L. M., Pan, J. J., Song, F. P., Sun,  
547 F. J., Wang, D. F., Wang, T. W., Wei, X. H., Wu, H. Q., Zhao, X., Zhou, Q., Zhang,  
548 G. L.: Significant loss of soil inorganic carbon at the continental scale, Natl. Sci.  
549 Rev., 9(2), <https://doi.org/10.1093/nsr/nwab120>, 2022.

550 R Core Team.: R: A language and environment for statistical computing, R Foundation  
551 for Statistical Computing, <https://www.R-project.org>, 2021.

552 Tang, C., Unkovich, M. J., Bowden, J. W.: Factors affecting soil acidification under  
553 legumes. III. Acid production by N<sub>2</sub>-fixing legumes as influenced by nitrate supply,  
554 New Phytol., 143(3), 513-521, <https://doi.org/10.1046/j.1469-8137.1999.00475.x>,  
555 1999.

556 Tatti, E., McKew, B. A., Whitby, C., Smith, C. J.: Simultaneous DNA-RNA extraction  
557 from coastal sediments and quantification of 16S rRNA genes and transcripts by  
558 real-time PCR, Jove-J. Vis. Exp., (112), <https://doi.org/10.3791/54067>, 2016.

559 Todd-Brown, K., Randerson, J. T., Post, W. M., Hoffman, F. M., Tarnocai, C., Schuur,  
560 E., Allison, S. D.: Causes of variation in soil carbon simulations from CMIP5 Earth  
561 system models and comparison with observations, Biogeosciences, 10(3), 1717-

1736, <https://doi.org/10.5194/bg-10-1717-2013>, 2013.

van Hees, P., Rosling, A., Essen, S., Godbold, D. L., Jones, D. L., Finlay, R. D.: Oxalate and ferricrocin exudation by the extramatrical mycelium of an ectomycorrhizal fungus in symbiosis with *Pinus sylvestris*, *New Phytol.*, 169(2), 367-377, <https://doi.org/10.1111/j.1469-8137.2005.01600.x>, 2006.

Ven, A., Verlinden, M. S., Fransen, E., Olsson, P. A., Verbruggen, E., Wallander, H., Vicca, S.: Phosphorus addition increased carbon partitioning to autotrophic respiration but not to biomass production in an experiment with *Zea mays*, *Plant Cell Environ.*, 43(9), 2054-2065, <https://doi.org/10.1111/pce.13785>, 2020.

Vicca, S., Goll, D. S., Hagens, M., Hartmann, J., Janssens, I. A., Neubeck, A., Penuelas, J., Poblador, S., Rijnders, J., Sardans, J., Struyf, E., Swoboda, P., van Groenigen, J. W., Vienne, A., Verbruggen, E.: Is the climate change mitigation effect of enhanced silicate weathering governed by biological processes? *Glob. Chang. Biol.*, 28(3), 711-726, <https://doi.org/10.1111/gcb.15993>, 2022.

Wang, B., Bao, Q., Hoskins, B., Wu, G. X., Liu, Y. M.: Tibetan plateau warming and precipitation changes in East Asia, *Geophys. Res. Lett.*, 35(14), <https://doi.org/10.1029/2008GL034330>, 2008.

Wang, G. X., Qian, J., Cheng, G. D., Lai, Y. M.: Soil organic carbon pool of grassland soils on the Qinghai-Tibetan Plateau and its global implication, *Sci. Total. Environ.*, 291(1-3), 207-217, [https://doi.org/10.1016/S0048-9697\(01\)01100-7](https://doi.org/10.1016/S0048-9697(01)01100-7), 2002.

Wang, J. P., Wang, X. J., Zhang, J., Zhao, C. Y.: Soil organic and inorganic carbon and stable carbon isotopes in the Yanqi Basin of northwestern China, *Eur. J. Soil Sci.*,

584 66(1), 95-103, <https://doi.org/10.1111/ejss.12188>, 2015.

585 Wild, B., Imfeld, G., Daval, D.: Direct measurement of fungal contribution to silicate  
586 weathering rates in soil, *Geology*, 49(9), 1055-1058,  
587 <https://doi.org/10.1130/G48706.1>, 2021.

588 Xiao, L. L., Lian, B., Hao, J. C., Liu, C. Q., Wang, S. J.: Effect of carbonic anhydrase  
589 on silicate weathering and carbonate formation at present day CO<sub>2</sub> concentrations  
590 compared to primordial values, *Sci. Rep.*, 5, <https://doi.org/10.1038/srep07733>,  
591 2015.

592 Yang, R. M., Yang, F.: Impacts of *Spartina alterniflora* invasion on soil inorganic  
593 carbon in coastal wetlands in China, *Soil Sci. Soc. Am. J.*, 84(3), 844-855,  
594 <https://doi.org/10.1002/saj2.20073>, 2020.

595 Yang, Y. H., Fang, J. Y., Ji, C. J., Ma, W. H., Su, S. S., Tang, Z. Y.: Soil inorganic  
596 carbon stock in the Tibetan alpine grasslands, *Global Biogeochem. Cy.*, 24,  
597 <https://doi.org/10.1029/2010GB003804>, 2010.

598 Yang, Y. H., Ji, C. J., Ma, W. H., Wang, S. F., Wang, S. P., Han, W. X., ... Smith, P.:  
599 Significant soil acidification across northern China's grasslands during 1980s-2000s,  
600 *Glob. Chang. Biol.*, 18(7), 2292-2300,  
601 <https://doi.org/10.1111/j.13652486.2012.02694.x>, 2012.

602 Yu, G. R., Jia, Y. L., He, N. P., Zhu, J. X., Chen, Z., Wang, Q. F., Piao, S. L., Liu, X.  
603 J., He, H. L., Guo, X. B., Wen, Z., Li, P., Ding, G. A., Goulding, K.: Stabilization  
604 of atmospheric nitrogen deposition in China over the past decade, *Nat. Geosci.*,  
605 12(6), 424, <https://doi.org/10.1038/s41561-019-0352-4>, 2019.

606 Zamanian, K., Pustovoytov, K., Kuzyakov, Y.: Pedogenic carbonates: Forms and  
 607 formation processes, *Earth-Sci. Rev.*, 157, 1-17,  
 608 <https://doi.org/10.1016/j.earscirev.2016.03.003>, 2016.

609 Zamanian, K., Zarebanadkouki, M., Kuzyakov, Y.: Nitrogen fertilization raises CO<sub>2</sub>  
 610 efflux from inorganic carbon: A global assessment, *Glob. Chang Biol.*, 24(7), 2810-  
 611 2817, <https://doi.org/10.1111/gcb.14148>, 2018.

612 Zamanian, K., Kuzyakov, Y.: Contribution of soil inorganic carbon to atmospheric CO<sub>2</sub>:  
 613 More important than previously thought, *Glob. Chang Biol.*, 25(1), E1-E3,  
 614 <https://doi.org/10.1111/gcb.14463>, 2019.

615 Zaharescu, D. G., Burghilea, C. I., Dontsova, K., Reinhard, C. T., Chorover, J.,  
 616 Lybrand, R.: Biological weathering in the terrestrial system, In *Biogeochemical*  
 617 *cycles* (pp. 1–32), 2020.

618 Zang, H. D., Blagodatskaya, E., Wen, Y., Xu, X. L., Dyckmans, J., Kuzyakov, Y.:  
 619 Carbon sequestration and turnover in soil under the energy crop *Miscanthus*:  
 620 repeated C-13 natural abundance approach and literature synthesis, *GCB Bioenergy*,  
 621 10(4), 262-271, <https://doi.org/10.1111/gcbb.12485>, 2018.

622 Zhou, Z. J., Li, Z. Q., Chen, K., Chen, Z. M., Zeng, X. Z., Yu, H., Guo, S., Shangguan,  
 623 Y. X., Chen, Q. R., Fan, H. Z., Tu, S. H., He, M. J., Qin, Y. S.: Changes in soil  
 624 physicochemical properties and bacterial communities at different soil depths after  
 625 long-term straw mulching under a no-till system, *SOIL*, 7, 595-609,  
 626 <https://doi.org/10.5194/soil-7-595-2021>, 2021.

627

## Figure captions

**Figure 1.** Soil inorganic C content, bulk density, and SIC density in the topsoil and subsoil. The horizontal solid and hollow lines inside each box represent medians and mean values, respectively. Significant differences between the topsoil and subsoil were inspected according to Tukey's test.

**Figure 2.** SIC density in relation to climatic, edaphic, plant, and microbial factors in the topsoil. The solid lines are fitted by ordinary least-squares regressions, and the shadow areas correspond to 95% confidence intervals. AM: alpine meadow; AS: alpine steppe; AD: alpine desert; MAP: mean annual precipitation; PAB: plant aboveground biomass; PC: plant coverage. The abbreviations for other variables are shown in Table 1.  $*p<0.05$ ;  $**p<0.01$ ;  $***p<0.001$ .

**Figure 3.** SIC density in relation to climatic, edaphic, plant, and microbial factors in the subsoil. The solid lines are fitted by ordinary least-squares regressions, and the shadow areas correspond to 95% confidence intervals. AM: alpine meadow; AS: alpine steppe; AD: alpine desert.

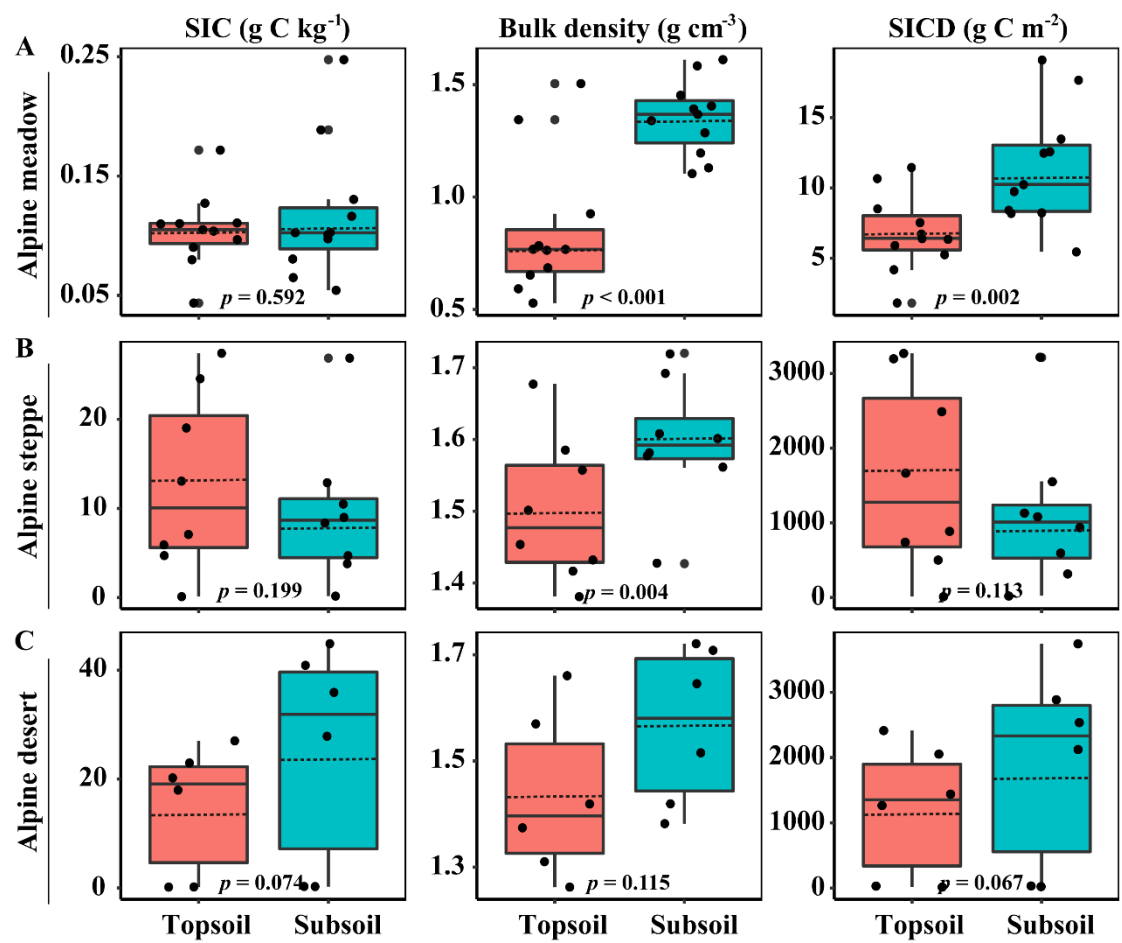
**Figure 4.** Relative effects of multiple drivers of SIC density in the topsoil (A) and subsoil(B). Climatic variables include MAP, MAT, and altitude; edaphic variables include pH, AN, and sand proportion; plant variables include PB, PC, and RB; microbial variables include MBC, BA, and FA.

**Figure 5.** Variation partitioning analyses (VPA) reveal the relative contribution of abiotic and biotic variables to SIC density in the (A) topsoil (61.2% vs. 84.4%) and (B) subsoil (73.4% vs. 86.1%), respectively. Results in three fractions: the unique effect of



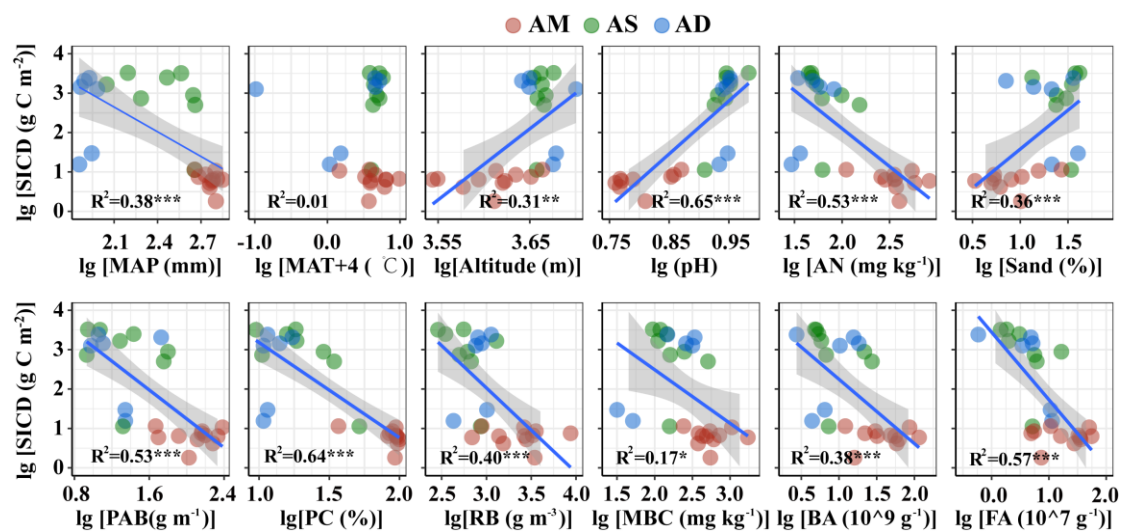
650 abiotic factors (X1), the unique effect of biotic factors (X2), and common interception  
651 of abiotic and biotic factors (X3).

652 **Figure 1.**  
653



654  
655

656 **Figure 2.**



658 **Figure 3.**

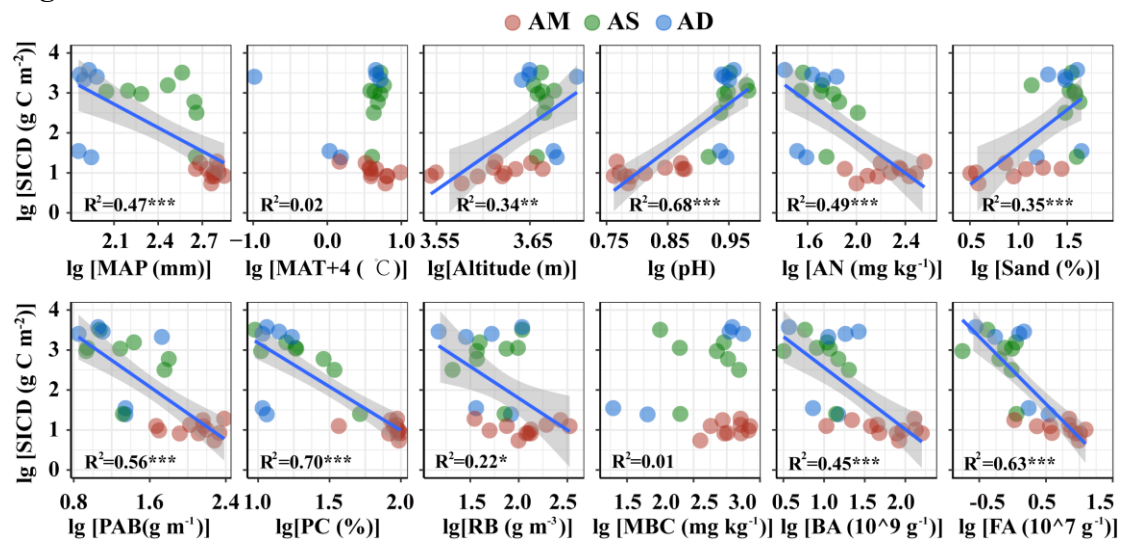
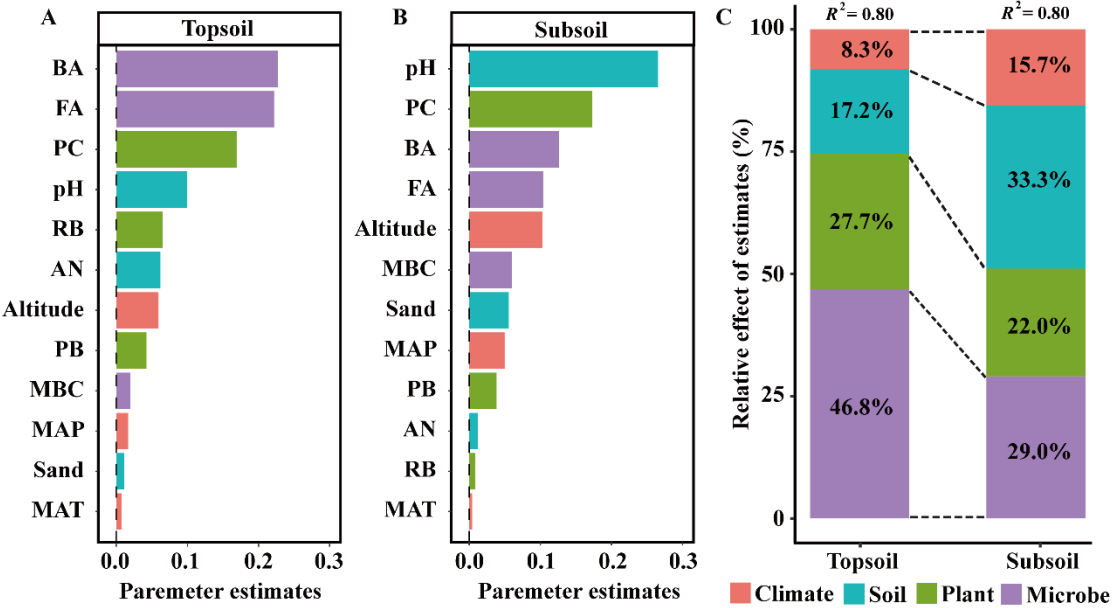
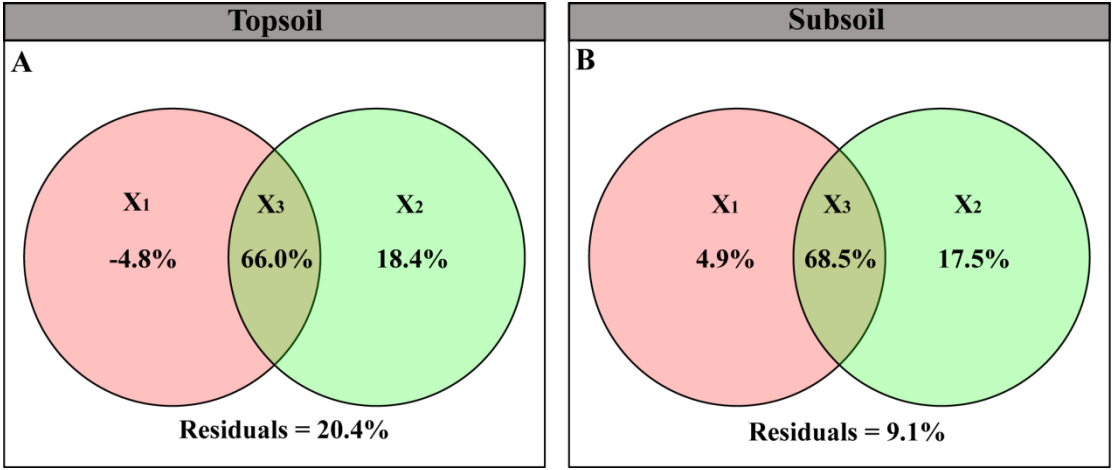


Figure 4.



664 **Figure 5.**



665

666

**Table 1.** Edaphic, plant, and microbial properties between the topsoil and subsoil for 25 sampling sites.

| Parameters  | Topsoil     | Subsoil     | <i>p</i> value |
|---|-------------|-------------|----------------|
| RB (g m <sup>-2</sup> )                               | 1670 ± 359  | 95.2 ± 15.3 | <0.001         |
| pH  | 7.66 ± 0.28 | 7.85 ± 0.26 | <0.001         |
| AN (mg kg <sup>-1</sup> )                             | 217 ± 43.7  | 131 ± 22.0  | 0.004          |
| SP (%)  | 47.1 ± 4.33 | 45.6 ± 4.87 | 0.698          |
| MBC (mg kg <sup>-1</sup> )                            | 385 ± 73.8  | 101 ± 9.7   | 0.001          |
| BA (10 <sup>9</sup> gene copies g <sup>-1</sup> soil) | 27.2 ± 5.68 | 12.6 ± 2.86 | 0.001          |
| FA (10 <sup>7</sup> gene copies g <sup>-1</sup> soil) | 14.2 ± 3.25 | 3.62 ± 0.84 | 0.001          |

RB: root biomass; AN: soil available nitrogen; SP: sand proportion; MBC: microbial biomass carbon; BA: soil bacterial abundance; FA: soil fungal abundance. Values are means ± standard error (SE). *p* values represent significant differences between the topsoil and subsoil according to Tukey's test.

673 **Supporting information**

674 Additional supporting information may be found online in the supporting information  
675 tab for this article.